



## Thick boron doped diamond single crystals for high power electronics<sup>☆</sup>

J. Achard<sup>a,\*</sup>, F. Silva<sup>a</sup>, R. Issaoui<sup>a</sup>, O. Brinza<sup>a</sup>, A. Tallaire<sup>a</sup>, H. Schneider<sup>b</sup>, K. Isoird<sup>b</sup>, H. Ding<sup>b</sup>, S. Koné<sup>b</sup>, M.A. Pinault<sup>c</sup>, F. Jomard<sup>c</sup>, A. Gicquel<sup>a</sup>

<sup>a</sup> LIMHP-CNRS, Université Paris 13, 99 avenue JB Clément, 93430 Villetaneuse, France

<sup>b</sup> LAAS-CNRS, Université de Toulouse, 7 Avenue Colonel Roche 31077 Toulouse, France

<sup>c</sup> GEMaC-CNRS, Université Versailles St-Quentin, 1 place Aristide Briand, 92195 Meudon Cedex, France

### ARTICLE INFO

#### Article history:

Received 19 April 2010

Received in revised form 7 November 2010

Accepted 15 November 2010

Available online 24 November 2010

#### Keywords:

Single crystal diamond growth

Boron doping

Thick films

Power electronic devices

Schottky diode

### ABSTRACT

Switch Mode Power Supply (SMPS) is now widely used for the control and conversion of electric power from one watt to several megawatts. In this context, the synthesis and use of wide bandgap semiconductor materials having physical characteristics superior to silicon is essential. Due to its outstanding physical properties (thermal conductivity, breakdown voltage, carrier mobilities...), diamond is a very promising material. However the success of its use in power electronics mostly relies on our ability to provide carriers by doping the material in a controlled manner. In particular the growth of thick heavily boron doped material is an essential requirement to develop vertical components which should allow, as it will be shown by modeling, limiting the series resistance of the devices in their on-state. Deposition conditions required to obtain high growth rate, high quality and heavily boron-doped material by plasma assisted chemical vapour deposition (MPACVD) will be described. It will be shown in particular that high growth rate, high-quality material, which is obtained at high microwave power density, comes at the expense of the boron concentration, and a compromise must be found. Preliminary results on boron doping of single crystal diamond will be presented and associated with electrical properties of pseudo-vertical Schottky Barrier Diodes (SBD). In particular, a critical electric field of 1.3 MV/cm has been demonstrated with a rectifying ratio of  $10^9$ . In the same time, current density close to  $1500\text{--}2000\text{ A cm}^{-2}$  has been reached, showing the potentiality of diamond for power-electronic applications.

© 2010 Elsevier B.V. All rights reserved.

### 1. Introduction

Since the Kyoto agreements, global warming has been a major concern and reducing the greenhouse gas emissions has become an essential objective among the developed countries. One of the key to success is to substitute fossil energies to sustainable energies such as wind turbines or solar cells, and to develop energy mixed solutions. This will imply to improve the electrical delivery systems and power converters in order to provide a more efficient conversion of their output power into a form that is suitable for grid connection. The generic term to refer to all such equipments is FACTS (Flexible AC Transmission Systems), which includes DC and AC transmission devices, stabilization of stream lines and distribution networks. Today's power systems are essentially based on silicon Insulated Gate Bipolar Transistor (IGBT), a mature technology that has little headroom for improvement. The low breakdown voltages of such devices requires to connect tens of them in series which, apart from the high-costs involved, makes the final system complex to control and run. Furthermore, due to the low operating limit temperature of silicon ( $150\text{ }^\circ\text{C}$ ) and its low thermal conductivity

( $150\text{ W m}^{-1}\text{ K}^{-1}$ ), these devices require large cooling systems. All of these constraints are still a barrier to the development of alternative energies.

In this context, the synthesis and use of wide bandgap semiconductor materials having physical characteristics superior to silicon, are very challenging. SiC and GaN are materials capable to outperform their silicon equivalents due to their higher thermal conductivities and breakdown voltages. Power electronic devices based on these materials are now undergoing a transition from research to commercial release. In comparison, diamond technology is still in its infancy. However this material possesses unrivalled properties [1] such as a groundbreaking thermal conductivity of  $2000\text{ W m}^{-1}\text{ K}^{-1}$  (5 times higher than copper) or a forecasted breakdown voltage of  $10\text{ MV cm}^{-1}$  (12 times that of silicon) that could drastically push the performance of the devices. Besides, high electron and hole mobilities in the range of  $2000\text{--}4500$  and  $1800\text{--}3800\text{ cm}^2\text{ V}^{-1}\text{ s}^{-1}$  at room temperature respectively [2–6], a low dielectric constant and a high chemical inertness that makes possible its use in very aggressive environments have been reported. Diamond definitely constitutes the ultimate material for power electronics.

Using microwave plasma assisted chemical vapour deposition (MPACVD), high quality and high purity monocrystalline diamond film can be deposited with mixtures of methane and hydrogen at moderate pressure. If the nitrogen background is kept below a few ppb, boron acceptor impurities with activation energy of 0.36 eV can be easily

<sup>☆</sup> Presented at NDNC 2010, the 4th International Conference on New Diamond and Nano Carbons, Suzhou, China.

\* Corresponding author. Tel.: +33 1 49 40 34 26.

E-mail address: [achard@limhp.univ-paris13.fr](mailto:achard@limhp.univ-paris13.fr) (J. Achard).

introduced by adding boron-containing precursors to the gas phase. Hole concentrations ranging from  $10^{16}$  to  $10^{21}$   $\text{cm}^{-3}$  can be achieved for different crystallographic orientations [7,8] but only over relatively small thicknesses for the highest doping levels. On the other hand, n-type doping is still a major issue since phosphorous, the only efficient donor, cannot be easily incorporated into a (100)-oriented crystal. Moreover its activation energy lies even deeper in the bandgap (0.6 eV) [9,10] which strongly limits the concentration of carriers at room temperature. Therefore, at first, elementary unipolar diamond-based devices will have to be considered for power electronics [11,12]. Various demonstrators have already been made (lateral Schottky diodes [13–17] or pseudo-vertical diodes [18–25]) showing the strong potential of diamond especially in terms of holding voltage. Unfortunately, in such structures, the forward polarization behaviour is not totally satisfactory because of the significant series resistance still limiting the current density.

In order to develop diamond-based high-voltage, high-current, and high-temperature electronics, several technological locks need to be overcome. In particular the fabrication of vertical components that allow significantly lowering the series resistance requires thick heavily boron doped diamond substrates. Some attempts in fabricating such structures have been made using high-pressure high-temperature (HPHT) boron-doped IIb diamond single crystals [26] but the high resistivity of such base substrates still hampers the performance of the device. This is mainly related to impurities incorporated in HPHT crystals such as nitrogen, chromium or nickel. More recently, Kumaresan et al. [27] have also fabricated a vertical Schottky diode using a CVD-grown diamond p+ substrate. Although high breakdown field was achieved, defects in the CVD layer have been pointed out as the main issue. In this work, the problem of the synthesis of thick heavily boron doped films by plasma assisted CVD is addressed.

In a first part, the simulation of different Schottky diode configurations will be described. It will be shown that vertical geometries are particularly interesting in the case of an operation at high currents which requires the use of large electrical contacts. In this type of geometry, thick films need to be used in order to provide sufficient mechanical strength for the device to be handled. In the perspective of an industrial development of such devices, it is thus essential to combine a high film quality with growth rates as high as possible, which can only be achieved using specific growth conditions. In a second part, the first experimental results obtained in terms of doping will be presented and growth conditions allowing the achievement of thick heavily boron doped films will be detailed. The last part will be more specifically dedicated to the fabrication process of diamond-based electronic devices. Characterisation of a first set of Schottky diodes will be presented. We will show that our results allow considering seriously the use of diamond for such applications.

## 2. Definition of the component geometry and constraints on the growth process

### 2.1. Component geometry

The main objective here is to define the requirements for the geometry and characteristics of boron-doped diamond films in order to fabricate an efficient Schottky diode. This type of devices must sustain a high-voltage (ideally above 10 kV) and allow a high current flow under forward bias. The latter necessarily requires having an on-state resistance ( $R_{\text{on}}$ ) as low as possible combined with a relatively large device surface. Indeed, if currents up to hundreds of Amps are expected, with a current density equal to  $5000 \text{ A cm}^{-2}$  then an area of  $2 \text{ mm}^2$  is imperative. Taking into account these dimensional constraints, only a vertical component geometry can be used – as usually done in silicon or SiC technology – because the section of the component is maximized to limit the series resistance.

This particular point is highlighted using simulation by comparing a pseudo-vertical and a vertical Schottky diode (see Fig. 1 and Table 1).

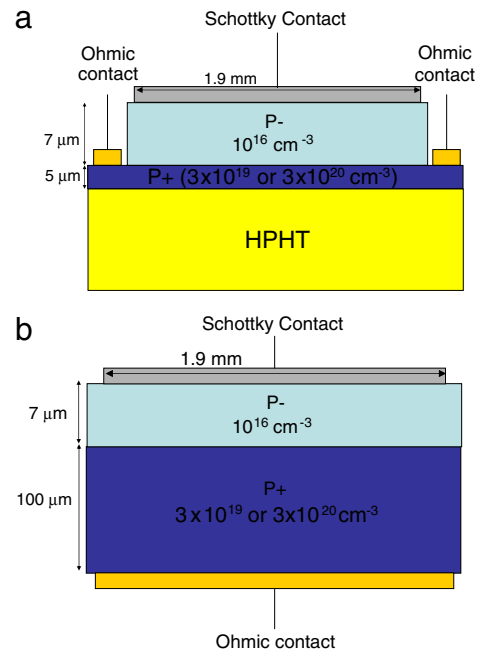


Fig. 1. Geometry of Schottky diodes used for the simulation. (a) pseudo-vertical diode; and (b) vertical diode. For the sake of clarity, drawings are not to scale.

The pseudo-vertical diode presented in Fig. 1a is fabricated on a  $5 \mu\text{m}$  thick p+ layer. Two doping values have been used for modeling the structure ( $3 \times 10^{19} \text{ cm}^{-3}$  and  $3 \times 10^{20} \text{ cm}^{-3}$ ). The Schottky contact is realised on a p– active layer doped at  $10^{16} \text{ cm}^{-3}$  and the contact length is 1.9 mm. A thickness of  $7 \mu\text{m}$  has been chosen in order to ensure a reverse voltage of 1.2 kV. Ohmic contacts are deposited on the p+ layer after etching of the p– layer. The vertical diode (Fig. 1b) is made on a  $100 \mu\text{m}$  thick p+ layer with an ohmic contact on the back side. p– and p+ layers have the same doping characteristics than for the pseudo-vertical structure. Starting from these two geometries,  $R_{\text{on}}$  has been calculated and the corresponding values are presented in Table 1.

From these results, it clearly appears that the use of a vertical structure allows reducing  $R_{\text{on}}$  by a factor of 4 to 5 depending on the temperature. Indeed, in this configuration, the conduction section (area through which current flows) is defined by the Schottky contact of the p– layer and the ohmic contact of the p+ layer as illustrated in Fig. 2a. Therefore,  $R_{\text{on}}$  is essentially due to the p– resistivity. In the pseudo-vertical configuration, current lines are confined in the  $5 \mu\text{m}$  thick p+ layer (see Fig. 2b) and the conduction section in the p+ layer is much lower than in the p– layer (Schottky contact area). In these conditions, the electrical resistance of the p+ layer becomes dominant.

The last point that can be highlighted is that, in a vertical configuration, the use of a lower doping ( $3 \times 10^{19} \text{ cm}^{-3}$  instead of  $3 \times 10^{20} \text{ cm}^{-3}$ ) has a lower influence on  $R_{\text{on}}$  than in a pseudo-vertical

Table 1  
Series resistance of pseudo vertical and vertical diodes calculated as a function of doping and thicknesses of p+ and p– layers at 300 K and 600 K.

	p– thickness ( $\mu\text{m}$ )	p– doping ( $\text{B cm}^{-3}$ )	p+ thickness ( $\mu\text{m}$ )	p+ doping ( $\text{B cm}^{-3}$ )	$R_{\text{on}}$ @ 300 K ( $\Omega$ )	$R_{\text{on}}$ @ 600 K ( $\Omega$ )
Pseudo-vertical diode	7	$10^{16}$	5	$3 \times 10^{19}$ $3 \times 10^{20}$	5.6 0.71	4.5 0.91
Verticale diode			100	$3 \times 10^{19}$ $3 \times 10^{20}$	0.23 0.21	0.17 0.16

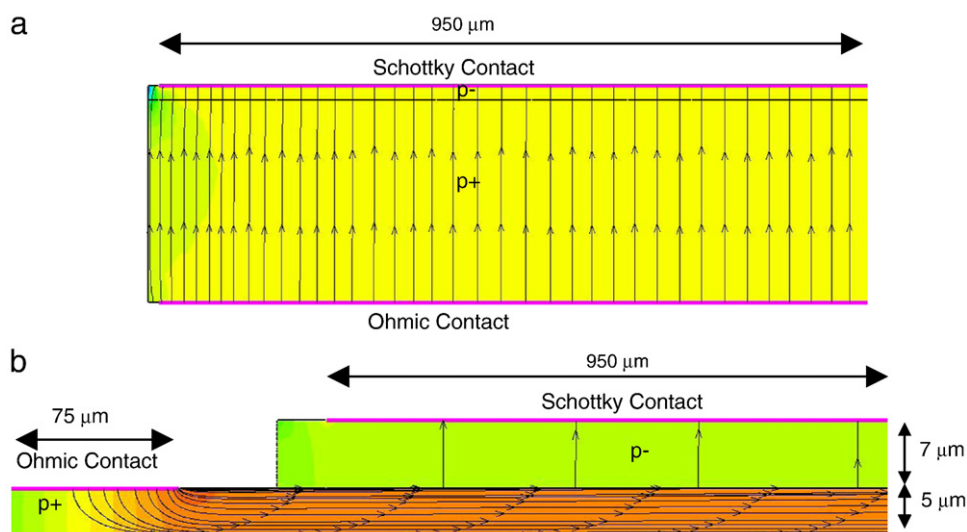


Fig. 2. Current lines distribution in the modelled structures. (a) Vertical diode; and (b) pseudo-vertical diode.

configuration. An increase of only 5% of  $R_{on}$  is calculated when doping is reduced by one decade. Indeed, in the case of a vertical structure, the large area of the component allows to accommodate more easily the decrease of doping. Thus, in this configuration, heavily doping of diamond is not absolutely required.

These results illustrate the importance of developing an appropriate process for growing thick boron-doped films in order to achieve vertical structures. In the perspective of an industrial development, the process should also involve growth rates as high as possible.

## 2.2. Constraints on the growth process

CVD diamond is obtained from gaseous precursors essentially composed of carbon and hydrogen, usually  $H_2$ - $CH_4$ . One of the key precursor species for growth is atomic hydrogen [28–31]. This chemical species is known to stabilize the diamond growing surface by saturating dangling bonds. It also leads to preferential etching of the non-diamond phases and to the creation of active sites on the one hand, and carbon containing precursors in the gas phase on the other hand, the latter also being essential for diamond growth. Therefore, it is highly desirable to increase as much as possible the atomic hydrogen density in the plasma if one wishes to improve both the growth rate and the diamond quality. Works conducted at LIMHP have clearly demonstrated that the efficient generation of atomic hydrogen relies on thermal dissociation of molecular hydrogen, a process occurring above gas temperatures of 3200 K [32–35].

Thus, only processes involving a strong activation of the gas phase to create the active species are able to provide both a gas temperature above 3200 K leading to growth rates of several microns per hour and sufficient control of the purity conditions for the manufacture of electronic-grade CVD diamond. High-power microwave cavity plasmas working at a moderate pressure satisfy these requirements. Microwave power density (MWPD), i.e. the ratio of the injected microwave power to the plasma volume<sup>1</sup>, which is a key parameter, must then be large enough to cause the thermal dissociation of molecular hydrogen. The results obtained from 1-D plasma models show that the maximum of the gas temperature is reached in the centre of the discharge (see Fig. 3) and therefore, the atomic hydrogen maximum is also located there [36,37].

<sup>1</sup> This quantity allows one to quantify the activation of the gas phase while also indirectly taking into account the working pressure. The plasma has been considered as a 4 cm diameter spherical ball corresponding to a 33 cm<sup>3</sup> volume.

The carbon growth species involved in diamond growth are essentially methyl radicals ( $CH_3$ ) [38–45]. The production of  $CH_3$  is governed by the chemical reaction  $CH_4 + H \rightarrow CH_3 + H_2$ . High  $CH_3$  density will therefore only be obtained if hydrogen dissociation (occurring at high gas temperatures) is efficient. However, too high a gas temperature leads to the conversion of these radicals into other carbon species [46–48]. The optimal gas temperature for the formation of  $CH_3$  radicals lies between 1500 and 2200 K. Nevertheless, since the substrate temperature is maintained around 1100 K, a temperature gradient exists between the hot plasma core and the substrate. Large amount of atomic hydrogen is then produced in the core of the discharge while a large methyl density exists near the substrate surface (see Fig. 3b and c).

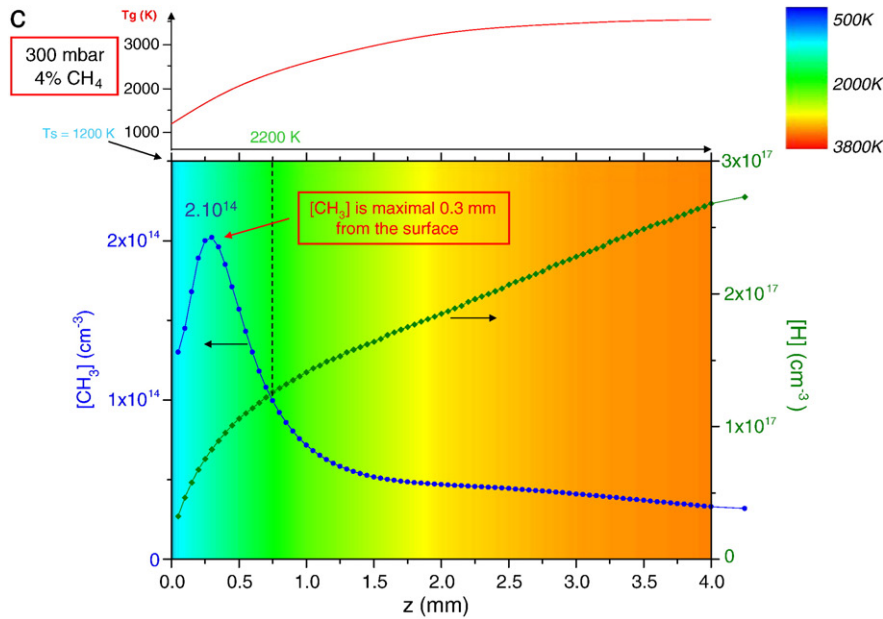
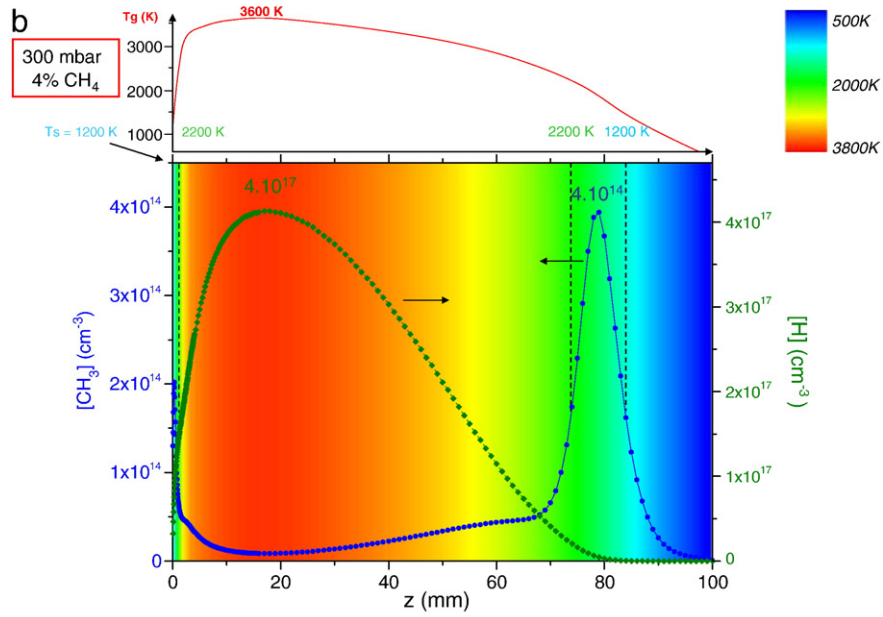
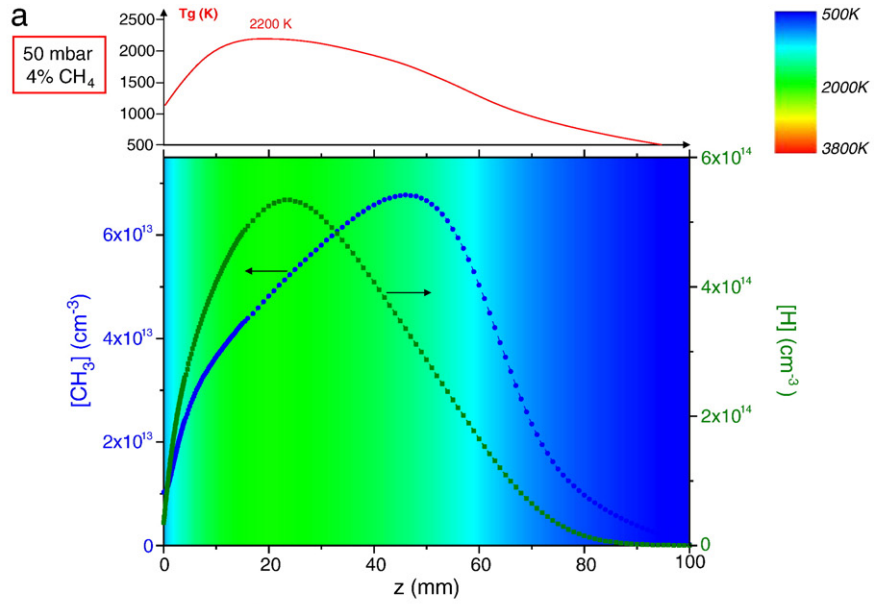
It is from the basis of these results that we have defined our plasma growth conditions for heavily boron doped diamond films. High MWPD is commonly used however, this plasma regime having been little explored [49] so far, for high boron doping.

## 3. Experimental results on boron doped diamond films

### 3.1. Influence of diborane concentration in the gas phase

Taking into account the previous part, a first set of samples has been elaborated. Depositions have been performed on  $3 \times 3 \times 1.5$  mm<sup>3</sup> HPHT Ib substrates. Before growth, all the substrates have been chemically cleaned in order to remove metallic and organic contaminants and have been submitted to a  $H_2/O_2$  plasma pre-treatment which benefits have already been demonstrated, especially in the case of thick film growth [50,51]. The reactor's microwave cavity has been designed at LIMHP in collaboration with Plassys company, in order to ensure optimal microwave coupling. This reactor is described in more details in ref. [52].

The MWPD has been fixed at 100 W cm<sup>-3</sup>, the substrate temperature at 850 °C and the methane concentration at 7%. The deposition time has been adjusted to obtain 20 μm thick films. These growth conditions correspond to our optimized conditions allowing the achievement of high quality intrinsic material in terms of purity, surface morphology and growth rate [53]. The  $[B]/[C]_{gas}$  ratio has been varied in the range 0.5 to 5000 ppm by adding  $B_2H_6$  in the gas phase. Boron incorporation in diamond as measured by SIMS is presented in Fig. 4 and shows a linear evolution up to 1000 ppm of  $[B]/[C]_{gas}$ .



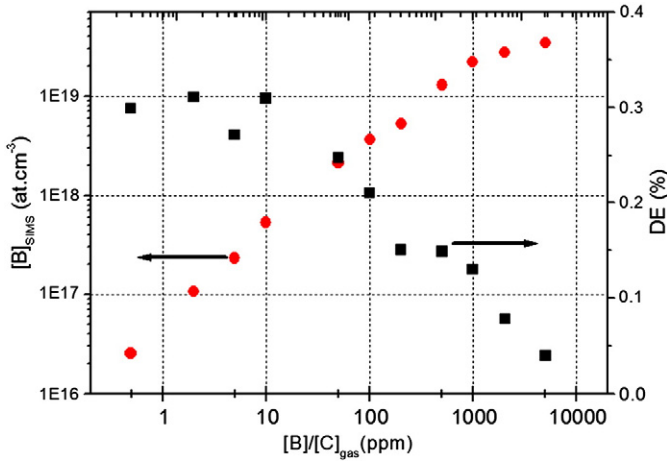


Fig. 4. Boron concentration in diamond measured by SIMS and doping efficiency as a function of [B]/[C]<sub>gas</sub> ratio.

Beyond this value, saturation is observed which is confirmed by a strong decrease of the doping efficiency (DE) defined in Eq. (1) as:

$$DE = \frac{[B] / [C]_{\text{diam}}}{[B] / [C]_{\text{gas}}} \quad (1)$$

where [B]/[C]<sub>diam</sub> is the ratio between the boron concentration (measured by SIMS) and the carbon concentration in the diamond film.

This trend has already been reported by Tokuda et al. [54] and attributed to an evolution of the plasma chemistry related to boron addition in the gas phase. Nevertheless, recent spectroscopic works carried out in our lab have shown that an increase of diborane in the gas phase up to 20,000 ppm does not modify neither electronic temperature nor gas temperature, these two parameters being well known to control plasma chemistry [55]. This trend is more likely to be related to the incorporation mechanism in the material. Indeed the number of incorporation sites available depends on the plasma conditions (H atom and CH<sub>3</sub> density) as well as the surface state of the diamond substrate (step edges, defects, etc.) and is limited. Above a certain value of [B]/[C]<sub>gas</sub>, boron incorporation does not linearly increase and shows some saturation. Another aspect could also be related to the surface morphologies which are usually improved by the presence of a large amount of boron, as will be detailed later. Because the presence of defects is well-known to favour impurities incorporation [56], the improvement in film morphologies may also prevent more boron from incorporating into the crystal lattice. Therefore in order to increase the boron concentration in the film and potentially reach the metallic transition, it is necessary to drastically increase the amount of diborane added to the gas phase. Unfortunately for [B]/[C]<sub>gas</sub> ratios above 5000 ppm the plasma is unstable due to the formation of soot that accumulate and prevent depositions longer than a couple of hours and therefore the growth of thick films.

### 3.2. Study of the influence of the MWPD on the growth of boron-doped diamond films

In the previous section, it has been shown that the use of high MWPD conditions is favourable to the rapid growth of high-quality single

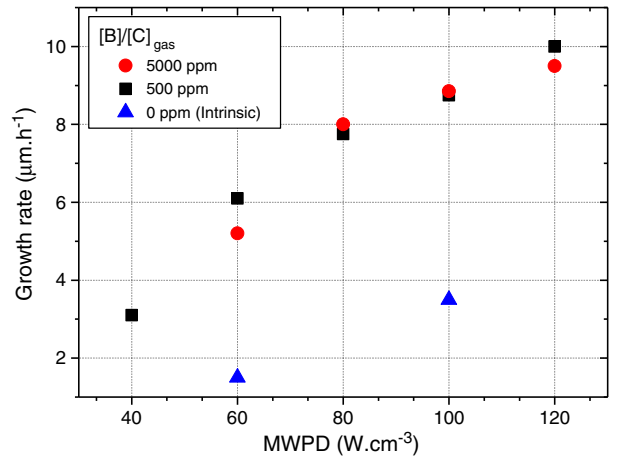


Fig. 5. Evolution of the growth rate as a function of MWPD using [B]/[C]<sub>gas</sub> of 500 and 5000 ppm. The growth rate of intrinsic material for two MWPD is also reported.

crystals. However in these conditions, the semiconductor-to-metal transition, which is desirable if one wants to fabricate vertical power devices, is not reached easily. This is mostly due to two main issues. Firstly, the boron incorporation tends to saturate at high [B]/[C]<sub>gas</sub> ratios to levels around  $3 \times 10^{19} \text{ cm}^{-3}$ . Secondly, the use of very large amounts of diborane (>5000 ppm) generates soot and makes the plasma unstable.

It should be noted here that the doping efficiencies obtained in these high MWPD conditions are usually much lower than those generally reported in the literature [54,57]. We partly attribute this effect to the high material quality as will be discussed later. The effect of the MWPD on boron incorporation has also so far never been reported.

In this study, we deposited boron-doped diamond films at MWPD varying from 40 to 120  $\text{W cm}^{-3}$ , and for two [B]/[C]<sub>gas</sub> ratios of 500 and 5000 ppm. Both the CH<sub>4</sub> concentration and the substrate temperature were maintained constant at 5% and 850 °C respectively. The growth rate of the deposited films is reported in Fig. 5.

The growth rate shows a strong increase from 3 to 10  $\mu\text{m/h}$  when the MWPD is increased from 40 to 120  $\text{W cm}^{-3}$ . This behaviour is consistent with the plasma studies reported previously. No relevant difference is observed between the films grown at [B]/[C]<sub>gas</sub> ratios of 500 and 5000 ppm. However in Fig. 5, the growth rate of 2 samples grown in similar conditions but using a reactor in which diborane has never been introduced is shown. It is surprising that the growth rate is lower by almost a factor of 3. A somehow similar effect has been reported with nitrogen impurities, since the use of a few ppm of this impurity is known to drastically speed up the deposition rates up to a factor of 10 [58,59]. Above a certain level though (a few hundreds of ppm) further addition of nitrogen does not affect the growth rate. In the case of boron, this effect seems to be lower since the growth rate is increased by a factor of 3 only. The mechanisms involved may therefore well be different.

Fig. 6a shows boron incorporation as a function of MWPD. It can be seen that for a given diborane amount introduced in the gas phase, the lower the MWPD, the higher the boron incorporation is. At 60  $\text{W cm}^{-3}$  and below, the semiconductor-to-metal transition is reached.

The origin of this DE drop at high MWPD (see Fig. 6b) is not fully understood. It can be partly attributed to the evolution of the chemical species in the plasma. Indeed, an increase of the MWPD is usually

Fig. 3. Gas temperature ( $T_c$ ), [CH<sub>3</sub>] and [H] calculation performed using a 1-D axial plasma model (the substrate is located at  $z = 0$ ) using 4% of CH<sub>4</sub> in the H<sub>2</sub>/CH<sub>4</sub> gas discharge and a substrate temperature of 1100 K. (a) Calculation performed at low MWPD (50  $\text{W cm}^{-3}$ ); (b) Calculation performed at high MWPD (200  $\text{W cm}^{-3}$ ) in a region between 0 and 100 mm from the substrate. (c) Zoom of (b) but in a region much closer to the substrate (0–4 mm).

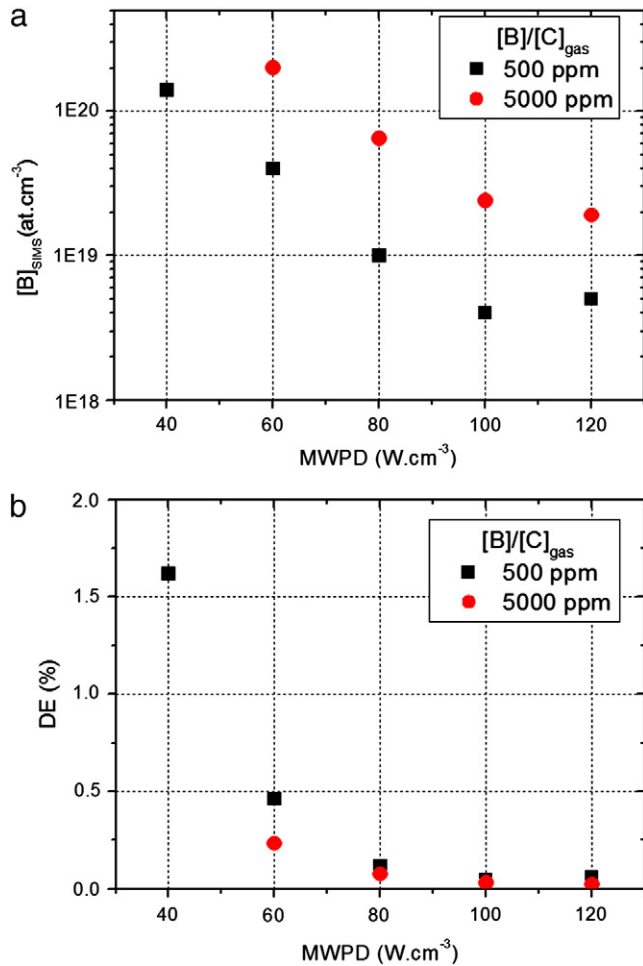


Fig. 6. Evolution of boron concentration measured by SIMS (a) and DE (b) as a function of MWPD for  $[B]/[C]_{gas}$  of 500 ppm and 5000 ppm.

accompanied by an increase of the gas temperature. The chemical reactions occurring in the plasma would therefore lead to a stronger dissociation of the BHx species. The chemical species involved in the incorporation of boron into the film could then be consumed, strongly limiting the DE. 1D plasma modeling as well as spectroscopy measurements are currently being performed in order to correlate these results with the species density in the plasma.

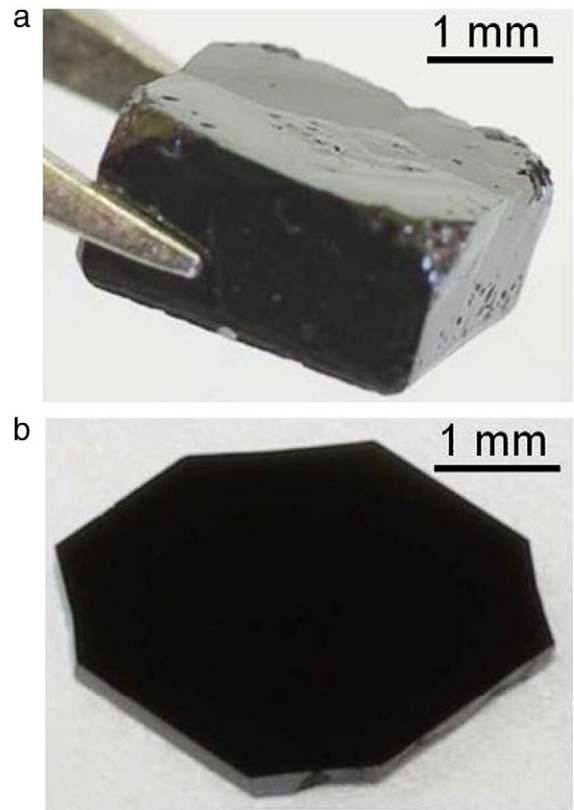


Fig. 8. (a) Boron doped film with its HPHT substrate before cutting and polishing. (b) Freestanding boron doped diamond film.

Another possibility can be due to the evolution of the diamond structure and the film quality which can modify boron incorporation efficiency. As a matter of fact, the surface morphologies of the grown films, reported in Fig. 7, show that for a  $[B]/[C]_{gas}$  ratio of 500 ppm, the morphology is strongly degraded by the use of low MWPD. The surface of the films is indeed covered with large pyramids on top of which unepitaxial crystals are found [60]. For MWPD of 100 W cm<sup>-3</sup> and above, the improvement of the surface morphology is related to the increase in atomic hydrogen in consistency with Refs. [61,62].

For a  $[B]/[C]_{gas}$  ratio of 5000 ppm, smooth surfaces are obtained in the whole MWPD range considered here indicating an improvement of the morphology by the addition of boron as described by Tokuda

MWPD (W.cm <sup>-3</sup> )	120	100	80	60	40
$[B]/[C]_{gas}$ 500 ppm					
$[B]/[C]_{gas}$ 5000 ppm					

Fig. 7. Influence of the MWPD on the surface morphology at 500 ppm and 5000 ppm of  $[B]/[C]_{gas}$ .

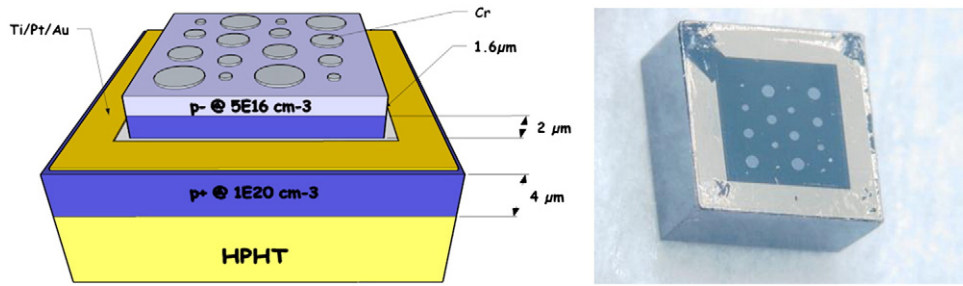


Fig. 9. Cross section and 3D photography of the fabricated SBD device structure.

et al. [54], but reported here for a wide range of MWPD. For the film deposited at  $40 \text{ W cm}^{-3}$  and 5000 ppm of  $[B]/[C]_{\text{gas}}$ , the boron concentration was so high that a dark graphite-containing layer was obtained which picture is not shown here.

From this study, it can be clearly concluded that although the use of lower MWPD strongly improves the DE thus limiting soot formation, it does not always allow keeping good morphologies. A good compromise was recently found by using a MWPD of  $60 \text{ W cm}^{-3}$  for a  $[B]/[C]_{\text{gas}}$  ratio of 5000 ppm, leading to the growth of a  $300 \mu\text{m}$ -thick heavily boron-doped film from which a freestanding plate has been sliced off as illustrated in Fig. 8.

**4. Fabrication and characterisation of pseudo-vertical Schottky diodes**

In parallel with the growth of thick heavily boron-doped films, a technology of Schottky diode fabrication, has been developed starting from thin boron-doped films in order to validate Schottky and ohmic contacts. Although a vertically designed diode has been found to be more relevant with regard to the forecasted power-devices, the geometry that has been chosen here is that of a pseudo-vertical diode (see Fig. 9). Indeed, this corresponds to a first attempt in order to optimize our fabrication process of Schottky diodes. In parallel, vertical diodes are being processed and results will be reported elsewhere. On a  $3 \times 3 \times 1.5 \text{ mm}^3$  Ib HPHT diamond substrate, a  $6 \mu\text{m}$ -thick heavily doped layer has been grown using a medium MWPD ( $50 \text{ W cm}^{-3}$ ,  $[B]/[C]_{\text{gas}}$  of 2000 ppm) to achieve the metal-to-semiconductor transition. A second layer has then been deposited in the same reactor choosing growth conditions allowing limiting boron incorporation (a few ppm of  $[B]/[C]_{\text{gas}}$  and  $100 \text{ W cm}^{-3}$ ).

A mesa structure of  $2 \times 2 \text{ mm}^2$  has then been fabricated at the centre of the sample by ICP etching, and Ti/Pt/Au ohmic contacts have been evaporated around the mesa structure on the heavily boron doped layer surface and subsequently annealed at  $500 \text{ }^\circ\text{C}$  for 1 h under nitrogen flow. Circular chromium contacts with different

diameters (100 and  $150 \mu\text{m}$ ) have finally been deposited on top of the mesa structure in order to obtain Schottky contacts.

*4.1. I–V characterisation at room temperature*

Typical I–V characteristics are presented in Fig. 10 for two diode diameters. From these curves, the main diodes parameters have been estimated (Table 2).

Rectifying ratios as high as  $10^{10}$ , associated with current densities reaching  $1500 \text{ A cm}^{-2}$  are demonstrated. Nevertheless, the reverse current is relatively high when the voltage reaches tens of volts. This behaviour is likely to be related to defects that can have various origins. Bulk defects can induce leakage paths in the material [63,64] and near surface homogeneously distributed defects across the contact area can also act electrically as highly doped and low barrier height regions [23].

Current–voltage measurements at reverse bias performed with the sample in air or immersed in an insulating liquid (fluorine FC40) are presented in Fig. 11. The insulating liquid avoids electric field crowding at Schottky contact edges causing premature breakdown of the device. A breakdown phenomenon in diamond is observed near  $-55 \text{ V}$  which corresponds to a breakdown electric field of  $1.3 \text{ MV cm}^{-1}$ , if a triangular field distribution within the uniformly doped p– layer is assumed [60]. This value is still below the theoretical predictions for

**Table 2**  
Diode characteristics estimated from the I–V curves.

Contact length of the diodes ( $\mu\text{m}$ )	Direct current $J_F$ ( $\text{A/cm}^2$ )	Reverse current $J_R$ ( $\text{A/cm}^2$ )	Rectifying ratio $J_F/J_R$	Threshold voltage $V_{th}$ (V)
100	1570	$10^{-7}$	$10^{10}$	1.9
150	980	$10^{-8}$	$10^{10}$	

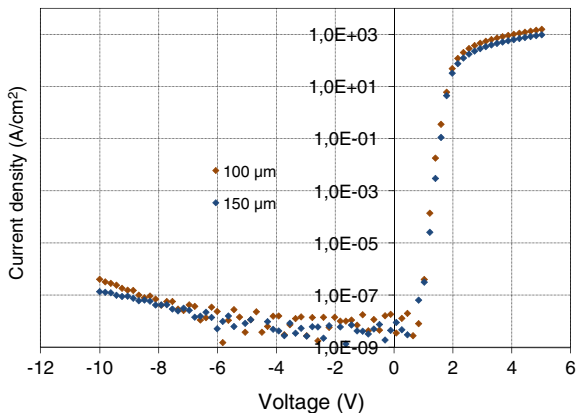


Fig. 10. I/V characteristics of Cr/diamond diodes for different contact lengths.

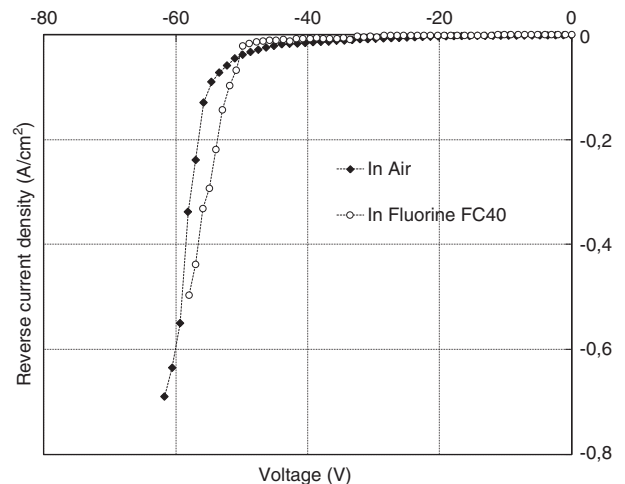


Fig. 11. Reverse I/V characteristic of Cr/diamond SBD in air and in fluorine FC 40.

diamond (10 MV/cm) which emphasizes on the challenges still remaining on diamond growth. Nevertheless, these results are very encouraging.

Through these different results, it has been shown that the technologies allowing the development of vertical Schottky are on their way although growth of heavily boron-doped freestanding films with low defect densities still needs to be improved.

## 5. Conclusion

Schottky diode modeling has shown that only a vertical component geometry can ensure high current operation (higher than 100 A). With such a geometry the on-state resistance ( $R_{on}$ ) can be decreased by a factor of 4 to 5. However this implies that the thick ( $> 100 \mu\text{m}$ ) highly boron doped ( $10^{20} \text{ cm}^{-3}$ ) diamond films are prepared so that they can mechanically robust to be separated from the substrate which is quite challenging.

The growth of thick films actually requires finding experimental conditions able to achieve high growth rate, high diamond purity and a good surface morphology. These conditions should involve high MWPD. However, above  $80 \text{ W cm}^{-3}$ , we have observed a strong reduction in doping efficiency, down to values as low as 0.01, limiting boron incorporation to a few  $10^{19} \text{ cm}^{-3}$ .

As a consequence, in order to compensate for the low DE, a very high diborane concentration should be used. Unfortunately this promotes soot formation and the deposition cannot be sustained for a long period of time. A compromise between the diamond quality, growth rate and soot formation in the gas phase led us to use medium MWPD of  $60 \text{ W cm}^{-3}$ . The first freestanding diamond plates were successfully obtained.

Technology for pseudo-vertical Schottky diodes fabrication has been validated showing encouraging I–V characteristics (current density between 1000 and  $2000 \text{ A cm}^{-2}$ , a rectifying ratio of  $10^{10}$  and a breakdown electric field in excess of  $1.3 \text{ MV cm}^{-1}$ ). This technology is now operational and the next step is the development of a vertical structure starting from the synthesized thick heavily boron doped free-standing films.

## Acknowledgements

This work was supported by French DGE project DIAMONIX, n° 08 2 90 6066.

## References

- [1] L.S. Pan, D.R. Kania, *Diamond: electronic properties and applications*, Kluwer Academic, Boston/Dordrecht/London, 1995.
- [2] J. Isberg, J. Hammersberg, E. Johansson, T. Wikstrom, D.J. Twitchen, A.J. Whitehead, S.E. Coe, G.A. Scarsbrook, *Science* 297 (2002) 1670.
- [3] J. Isberg, A. Lindblom, A. Tajani, D. Twitchen, *Phys. Stat. Sol. (a)* 202 (2005) 2194.
- [4] M. Nesladek, A. Bogdan, W. Deferme, N. Tranchant, P. Bergonzo, *Diamond Relat. Mater.* 17 (2008) 1235.
- [5] H. Pernegger, *Phys. Stat. Sol. (a)* 203 (2006) 3299.
- [6] J. Pernot, C. Tavares, E. Gheeraert, E. Bustarret, M. Katagiri, S. Koizumi, *Appl. Phys. Lett.* 89 (2006) 122111.
- [7] A. Deneuville, *Semicond. Semimet.* 76 (2003) 183.
- [8] A. Deneuville, C. Baron, S. Ghodbane, C. Agnes, *Diamond Relat. Mater.* 16 (2007) 915.
- [9] E. Gheeraert, N. Casanova, A. Tajani, A. Deneuville, E. Bustarret, J.A. Garrido, C.E. Nebel, M. Stutzmann, *Diamond Relat. Mater.* 11 (2002) 289.
- [10] M. Suzuki, S. Koizumi, M. Katagiri, H. Yoshida, N. Sakuma, T. Ono, T. Sakai, *Diamond Relat. Mater.* 13 (2004) 2037.
- [11] E. Kohn, M. Adamschik, P. Schmid, A. Denisenko, A. Aleksov, W. Ebert, *J. Phys. D* 34 (2001) R77.
- [12] A.Q. Huang, *IEEE Electron Device Lett.* 25 (2004) 298.
- [13] Y. Garino, T. Teraji, S. Koizumi, Y. Koide, T. Ito, *Phys. Stat. Sol. (a)* 206 (2009) 2082.
- [14] T. Teraji, Y. Koide, T. Ito, *Phys. Stat. Sol. (RRL)* 3 (2009) 211.
- [15] T. Teraji, Y. Garino, Y. Koide, T. Ito, *J. Appl. Phys.* 105 (2009) 126109.

- [16] T. Teraji, S. Koizumi, Y. Koide, T. Ito, *Appl. Surf. Sci.* 254 (2008) 6273.
- [17] T. Teraji, S. Koizumi, Y. Koide, T. Ito, *Jpn. J. Appl. Phys.* 46 (2007) L196.
- [18] J.E. Butler, M.W. Geis, K.E. Krohn, J. Lawless, S. Deneault, T.M. Lyszczarz, D. Flechtner, R. Wright, *Semicond. Sci. Technol.* 18 (2003) S67.
- [19] M. Brezeanu, S.J. Rashid, T. Butler, N.L. Rupesinghe, F. Udrea, K. Okano, G.A.J. Amarantunga, D.J. Twitchen, A. Tajani, C. Wort, *Electron. World Wireless World* 2 (2004) 20.
- [20] A. Aleksov, A. Vescan, M. Kunze, P. Gluche, W. Ebert, E. Kohn, A. Bergmaier, G. Dollinger, *Diamond Relat. Mater.* 8 (1999) 941.
- [21] A. Vescan, I. Daumiller, P. Gluche, W. Ebert, E. Kohn, *Diamond Relat. Mater.* 7 (1998) 581.
- [22] A. Vescan, I. Daumiller, P. Gluche, W. Ebert, E. Kohn, *IEEE Electron Device Lett.* 18 (1997) 556.
- [23] A. Vescan, W. Ebert, T. Borst, E. Kohn, *Diamond Relat. Mater.* 4 (1995) 661.
- [24] W. Ebert, A. Vescan, T.H. Borst, E. Kohn, *IEEE Electron Device Lett.* 15 (1994) 289.
- [25] H. Umezawa, K. Ikeda, R. Kumaresan, N. Tatsumi, S. Shikata, *IEEE Electron Device Lett.* 30 (2009) 960.
- [26] W. Huang, T.P. Chow, J. Yang, J.E. Butler, *Proceedings of the 17th International Symposium on Power Semiconductor Devices and IC's*, 2005, p. 319.
- [27] R. Kumaresan, H. Umezawa, S. Shikata, *Diamond Relat. Mater.* 19 (2010) 1324.
- [28] T.R. Anthony, *Vacuum* 41 (1990) 1356.
- [29] A.R. Badzian, T. Badzian, R. Roy, R. Messier, K.E. Spear, *Mater. Res. Bull.* 23 (1988) 531.
- [30] J.E. Butler, R.L. Woodin, *Philos. Trans. R. Soc. Lond. Ser. Math. Phys. Eng. Sci.* 342 (1993) 209.
- [31] F.G. Celii, J.E. Butler, *Appl. Phys. Lett.* 54 (1989) 1031.
- [32] K. Hassouni, T.A. Grotjohn, A. Gicquel, *J. Appl. Phys.* 86 (1999) 134.
- [33] K. Hassouni, S. Farhat, C.D. Scott, A. Gicquel, *J. Phys. III Fr.* 6 (1996) 1229.
- [34] A. Gicquel, M. Chenevier, Y. Breton, M. Petiau, J.P. Booth, K. Hassouni, *J. Phys. III* 6 (1996) 1167.
- [35] A. Gicquel, K. Hassouni, S. Farhat, Y. Breton, C.D. Scott, M. Lefebvre, *Diamond Relat. Mater.* 3 (1994) 581.
- [36] A. Gicquel, M. Chenevier, K. Hassouni, A. Tserepi, M. Dubus, *J. Appl. Phys.* 83 (1998) 7504.
- [37] M.A. Cappelli, T.G. Owano, A. Gicquel, X. Duten, *Plasma Chem. Plasma Process.* 20 (2000) 1.
- [38] J.C. Angus, A. Argoitia, R. Gat, Z. Li, M. Sunkara, L. Wang, Y. Wang, *Philos. Trans. R. Soc. Lond. A Phys. Sci. Eng.* 342 (1993) 195.
- [39] M.P. D'Evelyn, J.D. Graham, L.R. Martin, *Diamond Relat. Mater.* 10 (2001) 1627.
- [40] D.G. Goodwin, *J. Appl. Phys.* 74 (1993) 6888.
- [41] S.J. Harris, *Appl. Phys. Lett.* 56 (1990) 2298.
- [42] S.J. Harris, A.M. Weiner, *J. Appl. Phys.* 74 (1993) 1022.
- [43] W.L. Hsu, *Appl. Phys. Lett.* 59 (1991) 1427.
- [44] S. Skokov, B. Weiner, M. Frenklach, *J. Phys. Chem.* 98 (1994) 7073.
- [45] M. Tsuda, M. Nakajima, S. Oikawa, *J. Am. Chem. Soc.* 108 (1986) 5780.
- [46] K. Hassouni, O. Leroy, S. Farhat, A. Gicquel, *Plasma Chem. Plasma Process.* 18 (1998) 325.
- [47] A. Gicquel, M. Chenevier, Y. Breton, M. Petiau, J.P. Booth, K. Hassouni, *Journal de physique III* 6 (1996) 1167.
- [48] E.H. Wahl, T.G. Owano, C.H. Kruger, Y. Ma, P. Zalicki, R.N. Zare, *Diamond Relat. Mater.* 6 (1997) 476.
- [49] T. Teraji, K. Arima, H. Wada, T. Ito, *J. Appl. Phys.* 96 (2004) 5906.
- [50] F. Silva, J. Achard, X. Bonnin, A. Michau, A. Tallaire, O. Brinza, A. Gicquel, *Phys. Stat. Sol. (a)* 203 (2006) 3049.
- [51] A. Tallaire, J. Achard, F. Silva, R.S. Sussmann, A. Gicquel, E. Rzepka, *Phys. Stat. Sol. (a)* 201 (2004) 2419.
- [52] F. Silva, K. Hassouni, X. Bonnin, A. Gicquel, *J. Phys. Condens. Matter* 21 (2009) 364202.
- [53] J. Achard, A. Tallaire, R. Sussmann, F. Silva, A. Gicquel, *J. Cryst. Growth* 284 (2005) 396.
- [54] N. Tokuda, H. Umezawa, T. Saito, K. Yamabe, H. Okushi, S. Yamasaki, *Diamond Relat. Mater.* 16 (2007) 767.
- [55] M. Rayar, P. Supiot, P. Veis, A. Gicquel, *J. Appl. Phys.* 104 (2008) 033304.
- [56] P.M. Martineau, M.P. Gaukroger, R. Khan, D.A. Evans, *Phys. Stat. Sol. (c)* 6 (2009) 1953.
- [57] K. Ushizawa, K. Watanabe, T. Ando, I. Sakaguchi, M. Nishitani-Gamo, Y. Sato, H. Kanda, *Diamond Relat. Mater.* 7 (1998) 1719.
- [58] J. Achard, F. Silva, O. Brinza, A. Tallaire, A. Gicquel, *Diamond Relat. Mater.* 16 (2007) 685.
- [59] A. Tallaire, A.T. Collins, D. Charles, J. Achard, R. Sussmann, A. Gicquel, M.E. Newton, A.M. Edmonds, R.J. Cruddace, *Diamond Relat. Mater.* 15 (2006) 1700.
- [60] L.M. Tolbert, B. Ozpineci, S.K. Islam, M.S. Chinthavali, *Proc. Power and Energy Systems*, 2003, p. 317.
- [61] J. Achard, F. Silva, A. Tallaire, X. Bonnin, G. Lombardi, K. Hassouni, A. Gicquel, *J. Phys. D* 40 (2007) 6175.
- [62] T. Teraji, *Phys. Stat. Sol. (a)* 203 (2006) 3324.
- [63] R. Kumaresan, H. Umezawa, N. Tatsumi, K. Ikeda, S. Shikata, *Diamond Relat. Mater.* 18 (2009) 299.
- [64] H. Umezawa, N. Tokuda, M. Ogura, S.-G. Ri, S.-i. Shikata, *Diamond Relat. Mater.* 15 (2006) 1949.